Nanoscale

COMMUNICATION

View Article Online
View Journal | View Issue

Cite this: *Nanoscale*, 2016, **8**, 6490

Received 1st January 2016,
Accepted 26th February 2016

DOI: 10.1039/c6nr00014b

www.rsc.org/nanoscale

Site-specific conjugation of single domain antibodies to liposomes enhances photosensitizer uptake and photodynamic therapy efficacy†

M. Broekgaarden,‡[a] R. van Vught,‡[b] S. Oliveira,[c] R. C. Roovers,[c] P. M. P. van Bergen en Henegouwen,[c] R. J. Pieters,[d] T. M. Van Gulik,[a] E. Breukink[b] and M. Heger*[a]

Photodynamic therapy for therapy-resistant cancers will greatly benefit from targeted delivery of tumor photosensitizing agents. In this study, a strategy for the site-specific conjugation of single domain antibodies onto liposomes containing the photosensitizer zinc phthalocyanine was developed and tested.

Cancer is commonly treated with surgery, chemotherapy, radiotherapy, or combinations thereof. However, in the absence of a sufficient treatment response, patients rely on alternative methods to attain curation or palliation. One of the alternative treatments is photodynamic therapy (PDT), which has yielded promising clinical results in the treatment of various cancer types,[1] including non-resectable pancreaticobiliary cancers.[2,3] The therapy entails the administration of a photosensitizer that distributes throughout the body and accumulates non-selectively in the tumor mass. Subsequent irradiation of the tumor tissue with high-intensity light excites the photosensitizer, which transfers its energy to molecular oxygen to yield singlet oxygen in the process. Alternatively, excited photosensitizers transfer their excited electrons to oxygen to produce superoxide anion. Both types of reactive oxygen species (ROS) are capable of oxidizing biomolecules and, when produced excessively during PDT, induce lethal oxidative stress in light-exposed tumor cells.[4] Despite the notable therapeutic efficacy of PDT, its clinical implementation is restricted due to unfavorable pharmacokinetic properties of conventional photosensitizers, which gives rise to non-specific accumulation in the skin and associated adverse events such as skin phototoxicity.

To increase the specific delivery of photosensitizers to tumors, we have studied the feasibility of encapsulating the 2nd-generation photosensitizer zinc phthalocyanine (ZnPC) into liposomes intended for passive but specific photosensitizer delivery to tumor tissue *via* the tumor's enhanced permeability and retention (EPR) effect.[5] The experiments demonstrated that ZnPC-containing liposomes were photodynamically active and capable of inducing tumor cell death, despite limited cellular uptake.[6]

As an alternative or in addition to these passively targeted liposomes that localize extracellularly, immunotargeted liposomes may hold significant potential as the photosensitizing agents are delivered specifically to the target tissue and are released intracellularly. A variety of immunotargeted liposomes have been prepared for the selective delivery of doxorubicin to various malignancies,[7–9] and targeted modalities for PDT such as immunoconjugates, polyacrylamide nanoparticles, and polymeric micelles[10–13] have been investigated. However, the use of liposomes is advantageous over other drug delivery modalities as it has the capacity to simultaneously encapsulate hydrophobic and hydrophilic agents such as photosensitizers and adjuvant therapeutics. The rationale for co-encapsulating pharmacological adjuvants in photosensitizer-bearing liposomes has been explained in[1] and its utility proven in several recent papers.[14–16] Nevertheless, targeted liposomal drug delivery modalities have been sparsely investigated for application in PDT, despite promising *in vitro*[17–22] and *in vivo* findings.[23,24]

A major challenge for the immunotargeting of liposomes is the use of full length- or partial antibodies (55–150 kDa), which may be incompatible with liposomal preparation techniques,[25] or negatively affect the biodistributive behavior of the liposomes, which is largely governed by vesicle size.[26] Therefore, the use of highly (thermo)stable sdAbs derived from camelid immunoglobulins (also termed VHH, or nanobodies, 15 kDa) is an interesting alternative.[27]

[a]*Department of Experimental Surgery, Academic Medical Center, University of Amsterdam, Meibergdreef 9, 1105 AZ Amsterdam, The Netherlands. E-mail: m.heger@amc.uva.nl*
[b]*Department of Membrane Biochemistry and Biophysics, Institute of Biomembranes, Utrecht University, Padualaan 8, 3584 CH Utrecht, The Netherlands*
[c]*Division of Cell Biology, Science Faculty, Utrecht University, Padualaan 8, 3584 CH Utrecht, The Netherlands*
[d]*Department of Medicinal Chemistry and Chemical Biology, Utrecht Institute for Pharmaceutical Sciences, Utrecht University, P. O. Box 80082, NL-3508 TB Utrecht, The Netherlands*

†Electronic supplementary information (ESI) available: Materials and methods. See DOI: 10.1039/c6nr00014b

‡Equal contributions.

The aim of this study was to develop sdAb-functionalized, tumor-targeted liposomes (TTLs) by site-specifically conjugating EGa1 sdAbs against human epidermal growth factor receptor (EGFR, a growth-promoting cell surface receptor overexpressed by many tumor types[28]) onto ZnPC-containing liposomes. The sdAb's small size and relatively large surface area involved in antigen binding makes random conjugation to liposomal anchors potentially deleterious. Because the ligand binding site has a high likelihood to become obstructed during random conjugation, there is an urgent need for a more site-specific conjugation strategy.[29] To facilitate site-specific conjugation, a fusion protein composed of an anti-EGFR sdAb, an intein domain that can be cleaved with thiolating agents,[30] and an elastin-like polypeptide (ELP) was expressed in *Escherichia coli* BLR (DE3). The protein was purified by immobilized metal affinity chromatograpy and reversible precipitation of the ELP domain.[31] Subsequently, several thiolating compounds were explored for expressed protein ligation (ExPL) to yield a C-termin functionalized sdAb.

To determine whether site-specific labeling is more effective than random labeling in terms of binding affinity of the sdAb to the target ligand, the sdAb was cleaved from the fusion protein using either sodium 2-sulfanylethanesulfonate (MESNA, leaving a non-functional sulfonate) or cysteamine (CA, leaving a functional thiol). Following cleavage and purification, sdAb-MESNA was randomly conjugated to *N*-hydroxysuccinimide (NHS)-IRDye800 at primary amines (*e.g.*, N-terminus and side chains of Lys), whereas the sdAb-CA was more site-specifically conjugated to maleimide (Mal)-IRDye800 at the C-terminally introduced thiol (Fig. 1A). The ExPL rate constants (k) and plateaus were not significantly different between MESNA and CA (Fig. 1B and Table S1†). Both sdAbs were efficiently conjugated to 4 molar equivalents of IRDye800 (Fig. S1†). Subsequently, the binding affinity of sdAb-dye complexes was assessed on A431 cells under non-internalizing conditions (4 °C). With an equilibrium binding constant (K_d) of 29 nM, the site-specific conjugation yielded significantly tighter binding compared to random conjugation (K_d = 98 nM, p = 0.008) (Fig. 1C and Table S2†). Consequently, site-specific conjugation was employed in all subsequent experiments.

To assess whether site-specific conjugation of sdAbs to liposomes would lead to increased photosensitizer delivery, liposomes that were sterically stabilized with polyethylene glycol-Mal were prepared (summarized in Table S3†). The sdAb-CA was ligated to the lipid-anchored polyethylene glycol Mal on the liposomal surface (Fig. S2†), after which the Mal moieties on the liposome surface were blocked with β-mercaptoethanol (BME). Subsequently, liposomal uptake was determined in both EGFR-positive human epidermoid carcinoma (A431) cells and EGFR-negative 3T3 2.2 murine fibroblasts. The TTLs were selectively taken up by EGFR overexpressing cells as determined by fluorescence spectroscopy and confocal laser scanning microscopy (Fig. 2). The liposomes exerted no toxicity to either cell type (Fig. S3†).

The potential of TTLs to facilitate increased intracellular ZnPC delivery compared to non-targeted liposomes (NTLs) was investigated next. The TTLs were prepared with ZnPC in the lipid bilayer at a final ZnPC : lipid ratio of 0.003. A431 cells incubated with TTLs showed significantly higher ZnPC fluorescence compared to cells exposed to NTLs under similar conditions (Fig. 3A). Viability analysis showed that, despite

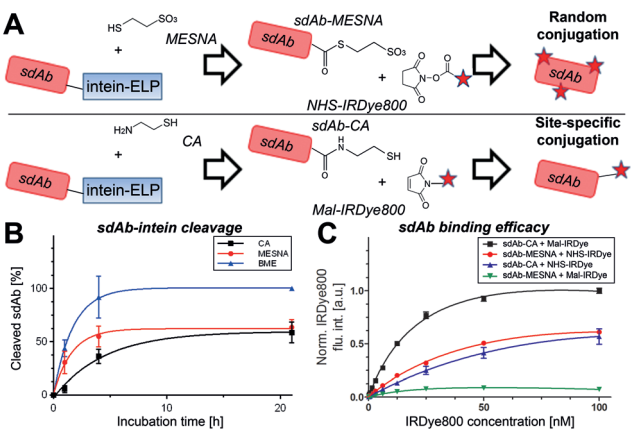

Fig. 1 (A) Schematic illustration of the thiol-mediated intein cleavage by MESNA and CA, and the subsequent NHS-mediated random conjugation of IRDye800 to the sdAb and the Mal-mediated site-specific conjugation of IRDye800 to the sdAb. (B) One phase exponential decay curves of the ExPL efficiency of CA, MESNA, and β-mercaptoethanol (BME, positive control). Data represent mean ± SEM of N = 3. (C) One site specific binding curves for nanobody-IRDye800 conjugate binding to A431 cells. All conjugations were done at a dye : antibody ratio of 4 : 1. The data were normalized to the highest IRDye800 fluorescence intensity obtained with 100 nM sdAb-CA + Mal-IRDye. Data represent mean ± SEM of N = 6.

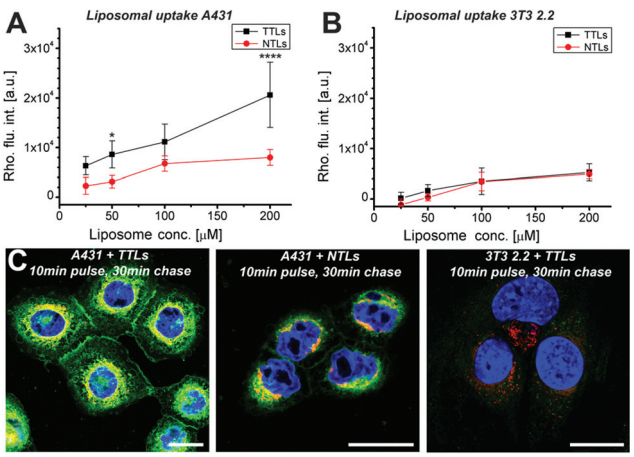

Fig. 2 Association of rhodamine (Rho)-labeled TTLs and Rho-NTLs with A431 cells (A) and 3T3 2.2 cells (B), plotted as a function of final lipid concentration. All data represent the mean ± SD of N = 6. Statistical analyses were performed with a one-way ANOVA and a Tukey's *post-hoc* test. (C) Confocal laser scanning microscopy of A431 and 3T3 2.2 cells after incubation with fluorescently (NBD)-labeled TTLs or NTLs. NBD (liposomes) is shown in green, MTR (mitochondria) is shown in red, and DAPI (nuclei) is shown in blue. Scale bar = 25 μm.

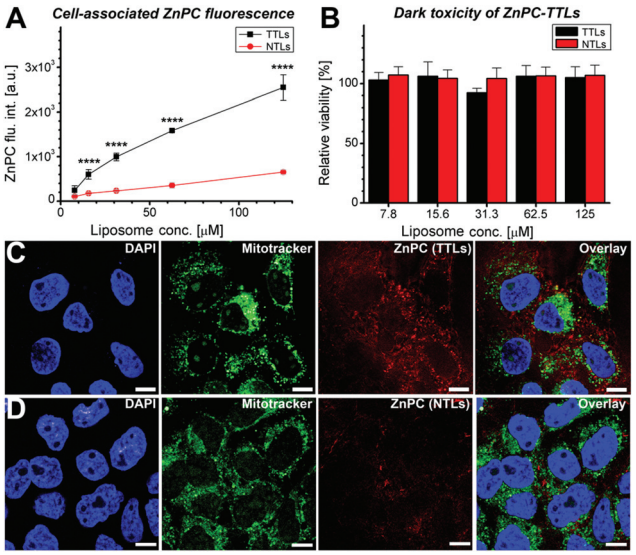

Fig. 3 (A) Extent of intracellular ZnPC delivery by TTLs and NTLs in A431 cells, plotted as a function of final lipid concentration. (B) Viability of A431 cells exposed to increasing concentrations of ZnPC-containing TTLs and NTLs in the absence of light irradiation (dark toxicity). All data represent the mean ± SD of $N = 6$. Statistical analyses were performed with a one-way ANOVA and a Tukey's *post-hoc* test. (C and D) Confocal laser scanning microscopy images of A431 cells incubated with TTLs (C) and NTLs (D). Cells were stained with DAPI (nuclei, blue) and MitoTracker (mitochondria, green). ZnPC as delivered by NTLs (C) and TTLs (D) is shown in red. Scale bar = 10 μm.

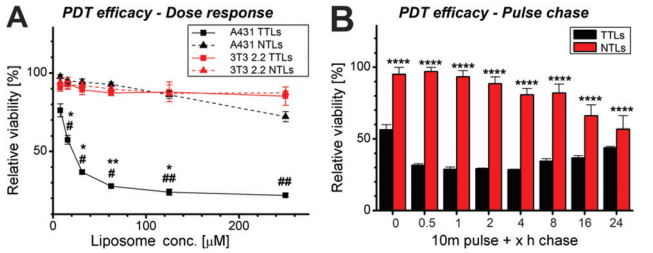

Fig. 4 (A) Relative viability of A431 and 3T3 2.2 cells after photosensitization with increasing concentrations of TTLs or NTLs and subsequent irradiation (10 J cm^{-2}). Data represent the mean ± SD of $N = 6$. Statistical testing was performed using a Kruskal–Wallis test and Dunn's multiple comparison analysis. Asterisks indicate differences between A431 cells incubated with TTLs and NTLs, pound signs indicate differences between the two cell lines undergoing similar treatment. (B) Relative viability of A431 cells after PDT after a 10 min exposure (pulse) to 125 μM TTLs or NTLs as a function of the drug-light interval (chase). Viability was assessed at 24 h post-PDT. All data represent the mean ± SD of $N = 6$. Statistical analysis was performed using a one-way ANOVA and Sidak's *post-hoc* test for multiple comparisons between the TTLs and NTLs.

exposure to the anti-EGFR sdAbs and increased ZnPC concentrations, there was no notable toxicity associated with TTLs in the absence of light irradiation (Fig. 3B). Although ZnPC is a relatively weak fluorophore, the increased ZnPC delivery into A431 cells following incubation with TTLs was confirmed by confocal laser scanning microscopy (Fig. 3C and D and Fig. S4†). Microscopy revealed a distinct localization pattern for ZnPC compared to NBD-labeled phospholipids (Fig. 2C), suggesting that ZnPC escapes the liposomes and distributes to organellar membranes following liposome internalization.

To determine whether the observed increased delivery of ZnPC to EGFR-positive cells by the TTLs would result in enhanced PDT, the PDT efficacy of TTLs was tested in A431 and 3T3 2.2 cells. Cells were incubated with 125 μM TTLs (final lipid concentration) for 10 min to allow binding, washed, incubated for 2 h to facilitate TTL uptake, and subsequently irradiated at a radiant exposure of 10 J cm^{-2}. Viability was assessed after 24 h. There was a dose-dependent relationship between the TTLs and PDT efficacy in A431 cells (Fig. 4A), which is in agreement with the uptake data (Fig. 2A and 3A). NTLs also exerted some PDT-induced cytotoxicity in A431 cells, albeit at substantially higher concentrations. Both NTLs and TTLs had no significant effect on 3T3 2.2 cells. Finally, we determined the effect of increasing drug-light intervals on PDT efficacy (125 μM TTLs) in pulse-chase experiments. A drug-light interval of 0.5 h increased the efficacy of PDT with TTLs, and this effect prevailed up to a drug-light interval of 4 h (Fig. 4B). At longer drug-light intervals, the efficacy of PDT decreased. This may have been caused by excretion of ZnPC from the cells, biotransformation of ZnPC, and/or time-dependent redistribution of ZnPC to organelles that trigger less extensive cell death signaling after PDT.[32] The NTLs exhibited increased PDT efficacy at longer drug-light intervals, implying that these liposomes did interact with the tumor cells during the 10 min incubation period but were internalized at a slower rate compared to TTLs. In summary, the ZnPC-loaded TTLs greatly enhanced the efficacy of PDT of EGFR-overexpressing cells compared to ZnPC-containing NTLs.

This study produced several important findings regarding immunotargeted liposomes. It was shown that site-specific conjugation of nanobodies to anchor molecules is beneficial over random NHS-based conjugation in terms of receptor binding efficacy. Moreover, sdAb-grafted liposomes exerted favorable and selective uptake characteristics and markedly increased PDT efficacy compared to NTLs. The latter is in agreement with prevailing literature on the uptake and therapeutic efficacy of immunotargeted liposomes as a drug delivery system.[32] Another interesting observation was that the liposomal ZnPC was not retained in the liposomes following cellular uptake, but distributed to different intracellular loci following uptake.

By fully utilizing the EPR effect to deliver TTLs to the tumor site, TTLs can subsequently be internalized by the tumor cells. This imparts a significant advantage over NTLs, which generally refrain from interacting with the tumor cells.[33] In this study, an sdAb against human EGFR receptor was utilized to bestow specific targeting properties upon the liposomes. EGFR is a tyrosine kinase receptor that is activated when EGF binds to its extracellular domain, resulting in a signaling cascade that stimulates proliferation and survival.[28] As such, EGFR is often overexpressed by tumors of varying origins, including

tumor types that are eligible for, but typically respond poorly to PDT. These include bladder tumors,[34] nasopharyngeal carcinoma,[35] and pancreaticobiliary cancers.[36,37] Inhibition of EGFR has also been shown to work in synergy with PDT to improve therapeutic efficacy,[38] thereby signifying the importance of a PDT regimen that targets EGFR-overexpressing cells.

Although immunotargeting to EGFR is clinically relevant, it should be emphasized that the nanobody used in this study can be exchanged to target different antigens and accommodate different cellular phenotypes. Additionally, the co-encapsulation and selective delivery of different hydrophobic and hydrophilic drugs is possible,[14–16,25] enabling a variety of potential applications for the liposome–nanobody conjugates described in this study.

Given the novelty of using sdAbs in combination with liposomal drug delivery, only few reports have appeared on the *in vivo* application of this modality. Although sdAb–liposome conjugates have therapeutic potential *in vivo*,[39,40] a comprehensive analysis of drug delivery efficacy in relation to non-targeted or mAb-functionalized liposomes has not been undertaken. With respect to conventional mAb-immunotargeted liposomes compared to non-targeted liposomes, both types of liposomes are typically equally effective with respect to tumor-specific accumulation *in vivo*, yet the immunotargeted liposomes generally display higher therapeutic efficacy.[8] It is believed that this enhanced therapeutic efficacy stems from the passive EPR-mediated leakage of liposomes followed by enhanced and specific uptake that is mediated by the subsequent interaction with surface receptors of the target cells. Although speculative, it is expected that sdAb–liposome conjugates display a similar biodistributive and therapeutic behavior *in vivo*.[27]

Overall, the use of targeted nanoparticulate drug delivery systems to achieve site-specific drug delivery has shown significant promise in the treatment of human disease such as cancer[41] and inflammatory disorders.[42] For instance, recent animal studies have demonstrated the potential of A7RC-targeted liposomes containing paclitaxel for the treatment of mammary tumors,[43] anti-cardiac troponin I-functionalized liposomes for the delivery of anti-miR-1 antisense oligonucleotides for the treatment of myocardial ischemia,[44] and *p*-aminophenyl-α-D-mannopyroside-modified liposomes for crossing the blood–brain barrier.[45] Additionally, targeted nanocarriers are gaining increased attention as multifunctional modalities used for theranostic applications.[46] As such, efficient means to obtain targeted nanocarriers to achieve spatially controlled delivery of therapeutic/diagnostic agents as described in the current study are of great value to the expanding field of nanoparticulate drug delivery.

Conclusions

With the aim to improve the selectivity of PDT, an efficient and feasible method was established to site-specifically conjugate sdAb's onto photosensitizer-containing liposomes for application in PDT. Following further *in vitro* and *in vivo* investigations, these liposomes may hold significant potential to enhance the efficacy of PDT of treatment-resistant solid cancers and ameliorate phototoxicity issues.

Acknowledgements

This work was funded by the Focus and Mass project (Utrecht University, Utrecht, the Netherlands) and the Dutch anticancer society (Stichting Nationaal Fonds tegen Kanker, Amsterdam, the Netherlands). The authors would like to thank Dr. Girgis Obaid and Dr. Jerrin Kuriakose (Wellman Center for Photomedicine, Massachusetts General Hospital and Harvard Medical School, Boston, MA) for useful discussions.

Notes and references

1 M. Broekgaarden, R. Weijer, T. M. van Gulik, M. R. Hamblin and M. Heger, *Cancer Metastasis Rev.*, 2015, **34**, 643–690.
2 T. Y. Lee, Y. K. Cheon and C. S. Shim, *Clin. Endosc.*, 2013, **46**, 38–44.
3 M. T. Huggett, M. Jermyn, A. Gillams, R. Illing, S. Mosse, M. Novelli, E. Kent, S. G. Bown, T. Hasan, B. W. Pogue and S. P. Pereira, *Br. J. Cancer*, 2014, **110**, 1698–1704.
4 A. P. Castano, P. Mroz and M. R. Hamblin, *Nat. Rev. Cancer*, 2006, **6**, 535–545.
5 H. Maeda, *Adv. Enzyme Regul.*, 2001, **41**, 189–207.
6 M. Broekgaarden, A. I. P. M. de Kroon, T. M. van Gulik and M. Heger, *Curr. Med. Chem.*, 2014, **21**, 377–391.
7 P. Sapra, E. H. Moase, J. Ma and T. M. Allen, *Clin. Cancer Res.*, 2004, **10**, 1100–1111.
8 C. Mamot, R. Ritschard, A. Wicki, G. Stehle, T. Dieterle, L. Bubendorf, C. Hilker, S. Deuster, R. Herrmann and C. Rochlitz, *Lancet Oncol.*, 2012, **13**, 1234–1241.
9 C. Hantel, F. Lewrick, S. Schneider, O. Zwermann, A. Perren, M. Reincke, R. Süss and F. Beuschlein, *J. Clin. Endocrinol. Metab.*, 2010, **95**, 943–952.
10 G. R. Reddy, M. S. Bhojani, P. McConville, J. Moody, B. A. Moffat, D. E. Hall, G. Kim, Y. E. Koo, M. J. Woolliscroft, J. V. Sugai, T. D. Johnson, M. A. Philbert, R. Kopelman, A. Rehemtulla and B. D. Ross, *Clin. Cancer Res.*, 2006, **12**, 6677–6686.
11 L. O. Cinteza, T. Y. Ohulchansky, Y. Sahoo, E. J. Bergey, R. K. Pandey and P. N. Prasad, *Mol. Pharmaceutics*, 2006, **3**, 415–423.
12 B. Q. Spring, A. O. Abu-Yousif, A. Palanisami, I. Rizvi, X. Zheng, Z. Mai, S. Anbil, R. B. Sears, L. B. Mensah, R. Goldschmidt, S. S. Erdem, E. Oliva and T. Hasan, *Proc. Natl. Acad. Sci. U. S. A.*, 2014, **111**, E933–E942.
13 A. M. Bugaj, *Photochem. Photobiol. Sci.*, 2011, **10**, 1097–1109.

14 M. Broekgaarden, R. Weijer, M. Krekorian, B. van den IJssel, M. Kos, L. K. Alles, A. C. van Wijk, Z. Bikadi, E. Hazai, T. M. van Gulik and M. Heger, *Nano Res.*, 2016, DOI: 10.1007/s12274-016-1059-0.
15 R. Weijer, M. Broekgaarden, M. Krekorian, L. K. Alles, A. C. van Wijk, C. Mackaaij, J. Verheij, A. C. van der Wal, T. M. Van Gulik, G. Storm and M. Heger, *Oncotarget*, 2015, **7**, 3341–3356.
16 B. Q. Spring, B. R. Sears, L. Z. Zheng, Z. Mai, R. Watanabe, M. E. Sherwood, D. A. Schoenfield, B. W. Pogue, S. P. Pereira, E. Villa and T. Hasan, *Nat. Nanotechnol.*, 2016, DOI: 10.1038/nnano.2015.311.
17 J. Morgan, A. G. Gray and E. R. Huehns, *Br. J. Cancer*, 1989, **59**, 366–370.
18 L. C. Bergstrom, I. Vucenik, I. K. Hagen, S. A. Chernomorsky and R. D. Poretz, *J. Photochem. Photobiol., B*, 1994, **24**, 17–23.
19 J. Morgan, H. Lottman, C. C. Abbou and D. K. Chopin, *Photochem. Photobiol.*, 1994, **60**, 486–496.
20 R. Rahmanzadeh, P. Rai, J. P. Celli, I. Rizvi, B. Baron-Lühr, J. Gerdes and T. Hasan, *Cancer Res.*, 2010, **70**, 9234–9442.
21 Y. Mir, S. A. Elrington and T. Hasan, *Nanomedicine*, 2013, **9**, 1114–1122.
22 S. Wang, G. Hüttmann, Z. Zhang, A. Vogel, R. Birngruber, S. Tangutoori, T. Hasan and R. Rahmanzadeh, *Mol. Pharm.*, 2015, **12**, 3272–3281.
23 T. A. Elbayoumi, S. Pabba, A. Roby and V. P. Torchilin, *J. Liposome Res.*, 2007, **17**, 1–14.
24 F. Yan, H. Wu, Z. Deng, H. Liu, W. Duan, X. Liu and H. Zheng, *J. Controlled Release*, 2015, **224**, 217–228.
25 S. Tangutoori, B. Q. Spring, Z. Mai, A. Palanisami, L. B. Mensah and T. Hasan, *Nanomedicine*, 2016, **12**, 223–234.
26 V. D. Awasthi, D. Garcia, B. A. Goins and W. T. Phillips, *Int. J. Pharm.*, 2003, **253**, 121–132.
27 S. Oliveira, R. Heukers, J. Sornkom, R. J. Kok and P. M. van Bergen en Henegouwen, *J. Controlled Release*, 2013, **172**, 607–617.
28 Y. Yarden and M. X. Sliwkowski, *Nat. Rev. Mol. Cell Biol.*, 2001, **2**, 127–137.
29 M. Kijanka, F. H. Warnders, M. El Khattabi, M. Lub-de Hooge, G. M. van Dam, V. Ntziachristos, L. de Vries, S. Oliveira and P. M. van Bergen en Henegouwen, *Eur. J. Nucl. Med. Mol. Imaging*, 2013, **40**, 1718–1729.
30 F. B. Perler, E. O. Davis, G. E. Dean, F. S. Gimble, W. E. Jack, N. Neff, C. J. Noren, J. Thorner and M. Belfort, *Nucleic Acids Res.*, 1994, **22**, 1125–1127.
31 W. Y. Wu, C. Mee, F. Califano, R. Banki and W. Wood, *Nat. Protoc.*, 2006, **1**, 2257–2262.
32 R. Weijer, M. Broekgaarden, M. Kos, R. Vught, E. A. J. Rauws, T. M. van Gulik, G. Storm and M. Heger, *J. Photochem. Photobiol. C: Photochem. Rev.*, 2015, **23**, 103–131.
33 X. Xu, W. Ho, X. Zhang, N. Bertrand and O. Farokhzad, *Trends Mol. Med.*, 2015, **21**, 223–232.
34 P. Lipponen and M. Eskelinen, *Br. J. Cancer*, 1994, **69**, 1120–1125.
35 T. J. Kim, Y. S. Lee, J.-H. Kang, Y.-S. Kim and C. S. Kang, *J. Surg. Oncol.*, 2011, **103**, 46–52.
36 D. Yoshikawa, H. Ojima, M. Iwasaki, N. Hiraoka, T. Kosuge, S. Kasai, S. Hirohashi and T. Shibata, *Br. J. Cancer*, 2007, **98**, 418–425.
37 T. Troiani, E. Martinelli, A. Capasso, F. Morgillo, M. Orditura, F. De Vita and F. Ciardiello, *Curr. Drug Targets*, 2012, **13**, 802–810.
38 M. G. del Carmen, I. Rizvi, Y. Chang, A. C. Moor, E. Oliva, M. Sherwood, B. Pogue and T. Hasan, *J. Natl. Cancer Inst.*, 2005, **97**, 1516–1524.
39 S. Oliveira, R. M. Schiffelers, J. van der Veeken, R. van der Meel, R. Vongpromek, P. M. van Bergen en Henegouwen, G. Storm and R. Roovers, *J. Controlled Release*, 2010, **145**, 165–175.
40 R. van der Meel, S. Oliveira, I. Altintas, R. Heukers, E. H. Pieters, P. M. van Bergen en Henegouwen, G. Storm, W. E. Hennink, R. J. Kok and R. M. Schiffelers, *Mol. Pharm.*, 2013, **10**, 3717–3727.
41 F. Fia, X. Liu, L. Li, S. Mallapragada, B. Narasimhan and Q. Wang, *J. Controlled Release*, 2013, **172**, 1020–1034.
42 U. Ikoba, H. Peng, H. Li, C. Miller, C. Yu and Q. Wang, *Nanoscale*, 2015, **7**, 4291–4305.
43 J. Cao, R. Wang, N. Gao, M. Li, X. Tian, W. Yang, Y. Ruan, C. Zhou, G. Wang, Z. Liu, S. Tang, Y. Yu, Y. Liu, G. Sun, H. Peng and Q. Wang, *Biomater. Sci.*, 2015, **3**, 1545–1554.
44 M. Liu, M. Li, S. Sun, B. Li, D. Du, J. Sun, F. Cao, H. Li, F. Jia, T. Wang, N. Chang, H. Yu, Q. Wang and H. Peng, *Biomaterials*, 2014, **35**, 3697–3707.
45 D. Du, N. Chang, S. Sun, M. Li, H. Yu, M. Liu, X. Liu, G. Wang, H. Li, X. Liu, S. Geng, Q. Wang and H. Peng, *J. Controlled Release*, 2014, **182**, 99–110.
46 H. Peng, X. Liu, G. Wang, M. Li, K. M. Brattle, E. Cochran and Q. Wang, *J. Mater. Chem. B*, 2015, **3**, 6856–6870.